DOI: 10.1002/ejic.200601120

Polymer-Supported Dioxido-Mo^{VI} Complexes as Truly Functional Molybdenum Oxotransferase Model Systems

Katja Heinze*[a] and Andreas Fischer[a]

Keywords: Enzyme models / Immobilised complexes / Molybdenum / Nitrogen ligands / Oxygen transfer

A truly functional model system for molybdenum oxotransferases provides evidence for all biologically realistic intermediates, namely mononuclear Mo^{VI}, Mo^{V} and Mo^{IV} species. Dinucleation to EPR-silent [Mo$^{V}_2$O$_3$] species prevailing in homogeneous solution is suppressed by immobilising the active species to a polymeric support by two-point attachment.

Introduction

Currently there is a great interest in structural and functional biomimetic models for active sites of metalloenzymes which mimic the primary coordination sphere (number and nature of ligating atoms) as well as the secondary coordination sphere (protein environment, site isolation, substrate selectivity, entatic state, secondary interactions with substrates, etc.).[1] Mononuclear molybdenum enzymes catalyse the net transfer of an oxygen atom between substrate and water [Equation (1)] shuttling between Mo^{VI}, Mo^{V} and Mo^{IV} states.[2,3]

$$X + H_2O \Leftrightarrow XO + 2H^+ + 2e^- \quad (1)$$

$$XO + Y \rightarrow X + YO \quad (2)$$

$$L_nMo^{VI}O_2 + L_nMo^{IV}O \rightarrow L_{2n}Mo^{V}_2O_3 \quad (3)$$

$$2\,L_nMo^{V}(OH)O \rightarrow L_{2n}Mo^{V}_2O_3 + H_2O \quad (4)$$

The primary oxo atom transfer (OAT) from/to molybdenum model compounds to/from substrates [Equation (2)] has been extensively investigated by Holm, Wedd, Young, Enemark, Basu and many others and is well understood.[4–7] The most successful model systems are based on enedithiolate ligands mimicking the natural sulfur ligation,[8–12] multidentate N/S ligands[13–17] and substituted hydrotris(pyrazolyl)borate ligands (Tp*, Tp^{iPr}).[18–21] Especially the latter family, although bearing no structural resemblance to natural enzymes, has been exceptionally useful for identifying mononuclear Mo^{V} species which are essential to the enzymatic catalytic cycle involving OAT and CEPT reactions (CEPT = coupled electron proton transfer). In these model systems the inherent tendency of molybdenum oxido complexes to form dinuclear species with a [Mo$_2$O$_3$] core via comproportionation [Equation (3)] or condensation [Equation (4)] is reduced due to steric hindrance. In molybdenum enzymes, the active site is located in the interior of the protein matrix and the substrate approaches the catalytic centre through a "funnel".[2,6] Of course dinucleation does not occur in natural systems.

[a] Anorganisch-Chemisches Institut der Universität Heidelberg, Im Neuenheimer Feld 270, 69120 Heidelberg, Germany
Fax: +49-6221-545707
E-mail: katja.heinze@urz.uni-heidelberg.de

Supporting information for this article is available on the WWW under http://www.eurjic.org or from the author.

Results and Discussion

The present report describes a different solution to the dinucleation problem, namely immobilisation of an active complex on a polymer support. In order to improve site-isolation and minimise leaching, the Mo complexes are immobilised onto the support via two-point fixation with two chelating 2-imino-pyrrolato ligands. The twofold attachment to the support parallels the incorporation of molybdenum in oxotransferases by pterin dithiolene and cysteinato ligands (e.g. sulfite oxidase or DMSO reductase).[2–7] Different EPR-active states have been observed in natural systems depending on preparation and environment.[2,3] The artificial system described below also shows several EPR-active Mo^{V} states during full biomimetic catalytic turnover [OAT and CEPT; Equation (1)]. First we introduce a sterically unencumbered model system, investigate the chemistry in homogeneous solution, and finally we describe our results for the immobilised system.

The soluble 2-imino-pyrrole ligand cleanly forms the bis(chelate) dioxido Mo^{VI} complex **1a** with MoCl$_2$O$_2$(dme) (Scheme 1). **1a** was fully characterised by NMR, IR and UV/Vis spectroscopic methods as well as mass spectrometric and elemental analysis (see Exp. Sect.). Reduction of **1a** with tertiary phosphanes results in OAT from the Mo^{VI} complex to the substrate giving the corresponding phosphane oxide (Scheme 2). Stoichiometric reaction with one

equivalent PPh_3 only produces 0.5 equiv. $OPPh_3$ even after prolonged reaction times as shown by time-dependent $^{31}P\{^1H\}$ NMR spectroscopy (Figure 1). Similar observations are made with PMe_3 as substrate albeit OAT proceeds faster in this case.[22] Thus comproportionation of Mo^{VI} and initially formed Mo^{IV} species to the diamagnetic μ-oxo species **2a** (Scheme 2) significantly slows down full conversion to Mo^{IV}. Complex **2a** has been analysed by mass spectrometry as well as NMR, IR and UV/Vis spectroscopy (see Exp. Sect.). The FAB and HR-FAB mass spectra confirm the dinuclear nature of the complex. A strong absorption band can be observed around 548 nm in the UV/Vis spectrum which is assigned the characteristic π-π* transition of the Mo–O–Mo unit. The antisymmetric Mo=O stretching vibration of the [O=Mo–O–Mo=O] core appears at 960 cm^{-1}.

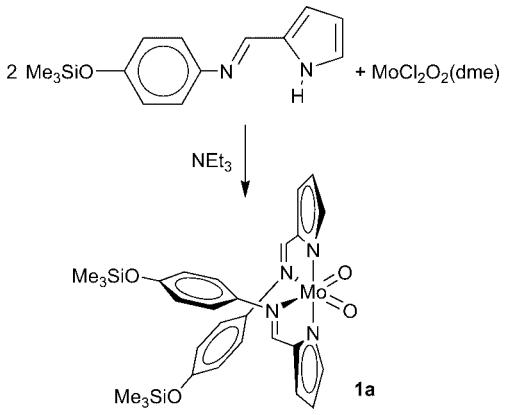

Scheme 1.

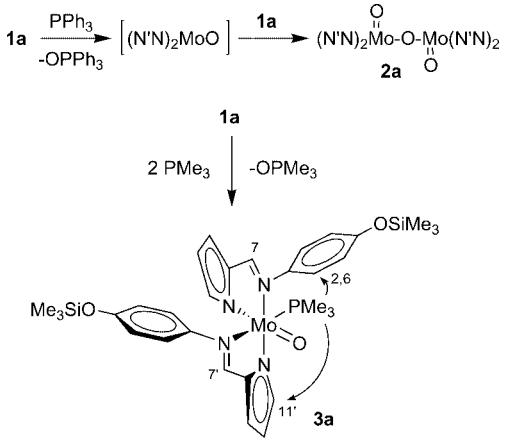

Scheme 2.

Full reduction of **1a** is achieved by using excess PMe_3 in THF at elevated temperature giving a green solution of the highly air-sensitive PMe_3 complex **3a** (Scheme 2). Coordination of PMe_3 to Mo^{IV} is shown by multinuclear two-dimensional NMR spectroscopy [$\delta(^{31}P) = 2.4$; $^2J_{PH} = 8.5$ Hz to methyl protons and $^4J_{PH} = 2.8$, <2 Hz to protons $H^{7'}$ and H^7 of the chelate ligands; Figure 2] and LIFDI mass spectrometry (*m*/*z* = 704, molecular ion peak[23]). In the NOESY spectrum NOE cross peaks are observed between

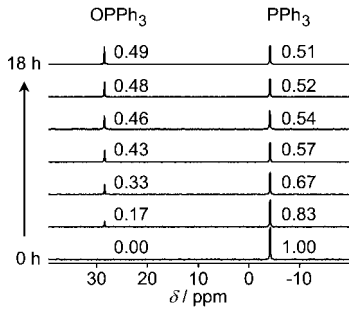

Figure 1. $^{31}P\{^1H\}$ NMR spectra of **1a** and 1 equiv. PPh_3 at 25 °C.

methyl protons of the PMe_3 ligand and protons of both chelate ligands ($H^{2,6}$ and $H^{11'}$) compatible with PMe_3 coordination *trans* to an imine nitrogen donor atom of one chelate ligand and *cis* to the imine nitrogen of the other (Scheme 2). Thus a second substrate can coordinate to molybdenum in the +IV state during OAT. Precedence for such a behaviour was only recently reported using a bis(η^2-pyrazolate)MoO_2 complex.[24]

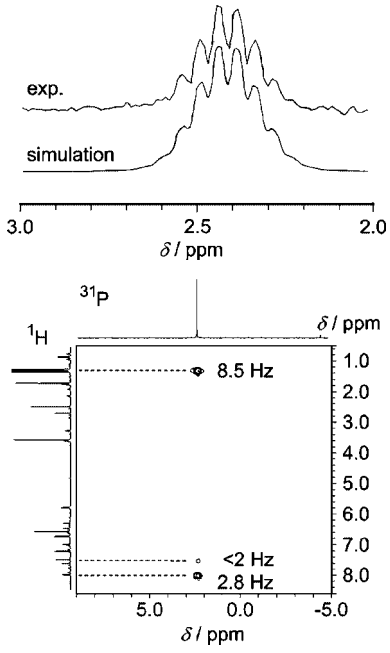

Figure 2. ^{31}P NMR spectrum and simulation (top) and PH-COSY spectrum of **3a** (bottom).

Re-oxidation of **3a** with DMSO as oxygen donor at 50 °C under single-turnover conditions yields dinuclear **2a** after 20 min and **1a** after 24 h. Thus a full OAT cycle [Equation (2)] from DMSO to PMe_3 has been accomplished with complex **1a**, however, with intermediate formation of dinuclear **2a** via comproportionation.

The reaction of **1a** with excess PMe_3 in THF (Scheme 2) was monitored UV-spectrophotometrically at 548 nm where **2a** possesses an absorption maximum (π-π* transition). Numerical simulation[25,26] of the data (Figure 3, top) yielded rate constants *k* for the rate-determining step (attack of PMe_3 at one oxido ligand of **1a**) and equilibrium constants *K* for the comproportionation [Equation (3)]. An Eyring

analysis yielded $\Delta H^{\neq}$ = 53 kJ mol^{-1} and $\Delta S^{\neq}$ = –82 J mol^{-1} K^{-1} (Figure 3, bottom). The negative activation entropy agrees with the associative transition state in the bimolecular reaction between **1a** and PMe_3.[4–7]

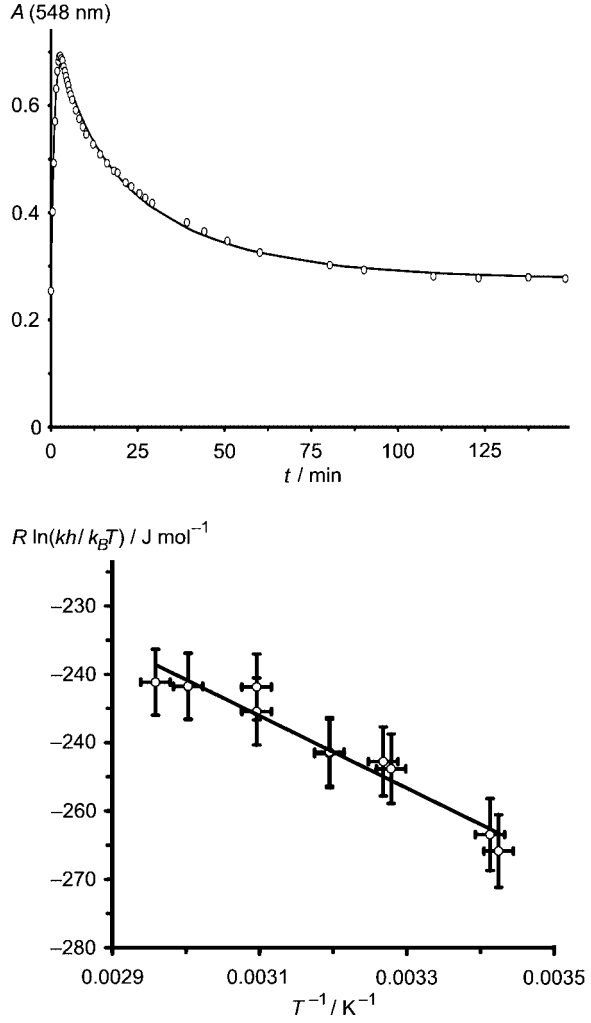

Figure 3. *A* vs. *t* plot of the reaction of **1a** and 100 eq PMe_3 at 60 °C (top) and Eyring plot (bottom).

So far it has been shown that oxo transfer chemistry (OAT) is possible with the system **1a/3a**. However, all attempts to observe mononuclear Mo^V species in homogeneous solution by EPR spectroscopy failed due to the high stability of EPR-silent **2a** towards disproportionation ($K_{dis} \approx 5 \cdot 10^{-6}$) and hydrolysis. To suppress (or at least diminish) formation of dinuclear species the doubly anchored versions of **1a/3a** are investigated (Scheme 3).

The immobilised bis(chelate) complex **1b** is prepared analogously to **1a** employing polymer-supported chelate ligands (Scheme 1 and Scheme 3; ligand loading 0.6–0.8 mmol g^{-1} polymer; polymer = polystyrene/2% divinylbenzene).[27–32] The amount of molybdenum incorporated by **1b** is compatible with the required 2:1 ligand/metal stoichiometry as shown by molybdenum uptake measurements.[23] Thus the molybdenum complexes are anchored to the polymeric backbone by two attachment points which should guarantee the desired site isolation effect (at least

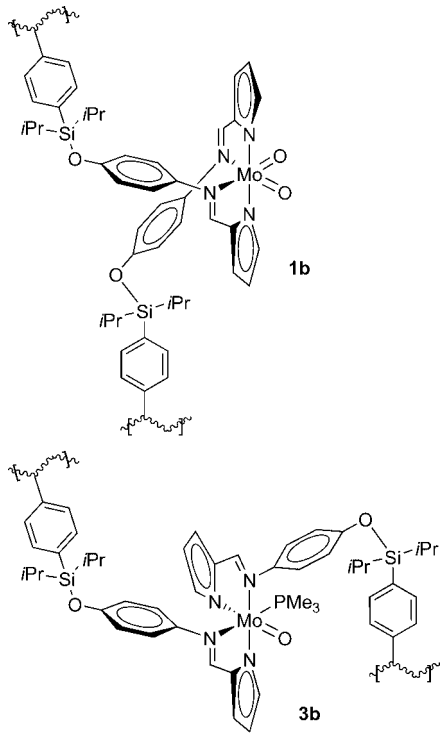

Scheme 3.

for some sites within the polymer). Cleaving the Si–O bonds of **1b** with fluoride ions releases the hydroxy analogue of **1a** into solution confirming the correct formation of **1b**.[27–32]

PMe_3 is oxidised by **1b** to $OPMe_3$ as shown by $^{31}P\{^1H\}$ NMR spectroscopic analysis of the solution. The reduction product of **1b** is the immobilised PMe_3 complex **3b** (Scheme 3) characterised by its CP MAS $^{31}P\{^1H\}$ NMR signal at δ = 2.4 which fits to that observed for the soluble complex **3a** (Figure 2 and Figure 4).

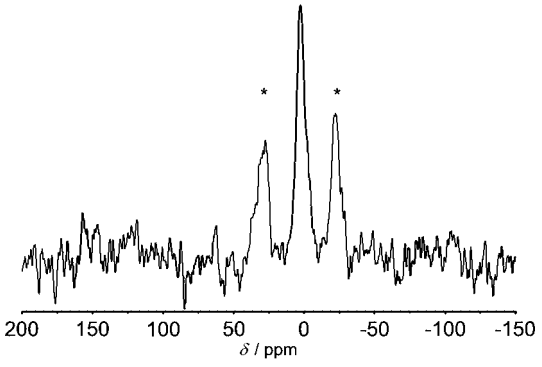

Figure 4. CP MAS $^{31}P\{^1H\}$ NMR spectrum (4 kHz) of **3b** (* denote rotational side bands).

The anchored Mo^{VI} and Mo^{IV} complexes **1b** and **3b** were subjected to one-electron reduction and oxidation, respectively (CEPT chemistry). Reaction of **1b** with cobaltocene $Co(C_5H_5)_2$[33] gave polymer **4b** which is EPR-active. Anisotropic EPR spectra (g_1 = 1.9544, g_2 = 1.9388, g_3 = 1.9111; **1b** and **3b** are EPR-silent) both in the solid and the THF gel-phase of the polymer are observed at room temperature (Figure 5). We have previously shown that singly polymer

attached Cu^{II} complexes give isotropic EPR spectra under gel-phase conditions suggesting that a single-point attachment allows for sufficient mobility.[34] However, two-point fixation seems to decrease the mobility of the anchored complexes **4b** resulting in anisotropic EPR spectra even in the gel-phase at room temperature.[35] In addition this finding proves that the molybdenum species are still bound to the support as otherwise isotropic signals for soluble species would have been observed.

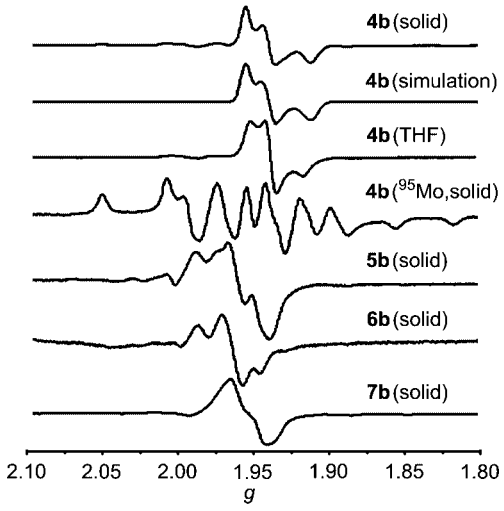

Figure 5. EPR spectra of **4b**–**7b** (295 K, 9.4 GHz).

All *g*-values observed for **4b** are well below 2.0 typical for Mo^{V} species with non-thiolate donor atoms. Further confirmation of mononuclear Mo^{V} present is provided by using ^{95}Mo-enriched precursors (98%; $I = {}^{5}/_{2}$). The isotopically enriched polymer **4b** displays characteristic anisotropic hyperfine coupling to the ^{95}Mo nucleus in the EPR spectrum (Figure 5). Upon one-electron reduction of **1b** an anionic dioxido-Mo^{V} species should be formed initially. For $[MoO_2(NCS)Tp^*]^-$ an anisotropic spectrum (*g*-values of 1.9939, 1.9277, 1.8350) is observed at 77 K, while the corresponding protonated complex MoO(OH)(NCS)Tp* displays signals at $g = 1.966$, 1.944 and 1.922 much more similar to the values observed for **4b**.[21] Addition of a proton source (HBF_4) to the reduced polymer **4b** had no influence on the EPR spectrum, suggesting that **4b** has already captured a proton. However, if protonation to the hydroxo complex occurred during reduction split signals due to coupling to the hydroxo proton are expected which is not observed for **4b**.[21] The protonation state of **4b** remains ambiguous at the moment.

One-electron oxidation of the anchored Mo^{IV} complex **3b** with $[Fe(C_5H_5)_2][PF_6]$[33] yields polymer **5b**. Again ^{95}Mo labelling proves the presence of Mo^{V} species.[23] The EPR pattern of **5b** differs from that of **4b** as additional coupling to an $I = {}^{1}/_{2}$ nucleus is observed ($g_1 = 1.9812$, $g_2 = 1.9528$, $g_3 = 1.9415$; $A_1 = 23$ G, $A_2 = 27$ G, $A_3 = 23$ G; Figure 5). Thus it is suggested that PMe_3 (^{31}P: $I = {}^{1}/_{2}$) is still bound to molybdenum in the +V state. PMe_3 coordinated to Mo^{V} should only be weakly bound so that ligand displacement reactions should be possible.

Indeed, reaction of **4b** with water displaces the phosphane and generates the Mo^{V}-containing polymer **6b**. The EPR spectrum of **6b** could only be reasonably simulated with two equivalent $I = {}^{1}/_{2}$ nuclei present ($g_1 = 1.9868$, $g_2 = 1.9624$, $g_3 = 1.9440$; $A_1 = 30$ G, $A_2 = 7$ G, $A_3 = 28$ G; Figure 5).[23] We tentatively assign these nuclei to two protons of a coordinated water molecule (or less likely to two hydroxo ligands). Substitution of PMe_3 is also possible with chloride ions ($[nBu_4N]Cl$) giving polymer **7b**. The EPR spectrum of **7b** can be simulated with coupling to one Cl nucleus (^{35,37}Cl: $I = {}^{3}/_{2}$; $g_1 = 1.9680$, $g_2 = 1.9522$, $g_3 = 1.9362$; $A_1 = 7$ G, $A_2 = 10$ G, $A_3 = 8$ G; Figure 5).[39] Thus different ligands (substrate, water, chloride) can occupy the free coordination site at Mo^{V} as suggested by the different EPR spectra – similar to the situation assumed in molybdenum enzymes.[2] Remarkably, no evidence for leaching was observed during all these operations (reduction, oxidation, ligand exchange).

A full catalytic cycle (OAT and CEPT) involving PMe_3 as oxygen acceptor, $[Fe(AcC_5H_4)_2][BF_4]$ as one-electron oxidant,[33] water as oxygen donor and phosphazene base P_1-*t*Bu[36] as proton acceptor is finally attempted. $[Fe(AcC_5H_4)_2][BF_4]$ is employed instead of $[Fe(C_5H_5)_2][BF_4]$ because of its higher oxidation potential.[33] A suggested mechanism is depicted in Scheme 4. In fact, under these conditions **1b** catalysed the production of 25 equiv. $OPMe_3$ from PMe_3, water and oxidant within 48 h as shown by $^{31}P\{^{1}H\}$ NMR spectroscopy (Figure 6). With ^{18}O-enriched water the label is incorporated into $OPMe_3$ as shown by mass spectrometric analysis. This proves that water is the source of the oxygen atom in the phosphane oxide product as required [Equation (1)].[23]

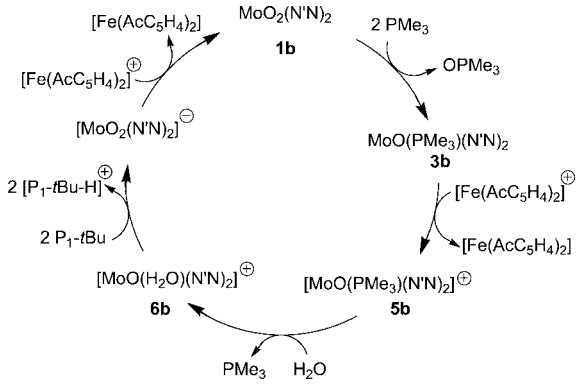

Scheme 4.

Although the present system definitely does not represent a structural model (Mo enzymes prefer sulfur coordination[2]) it is a truly functional model providing evidence for all biologically realistic mononuclear intermediates, namely Mo^{VI}, Mo^{V} and Mo^{IV} species. Dinucleation to EPR-silent $[Mo^{V}_2O_3]$ species prevailing in homogeneous solution and inhibiting CEPT chemistry is largely suppressed when the active species are doubly bound to a polymeric support. Double anchoring of active pre-catalysts to polymeric matrices with the aim to detect reactive interme-

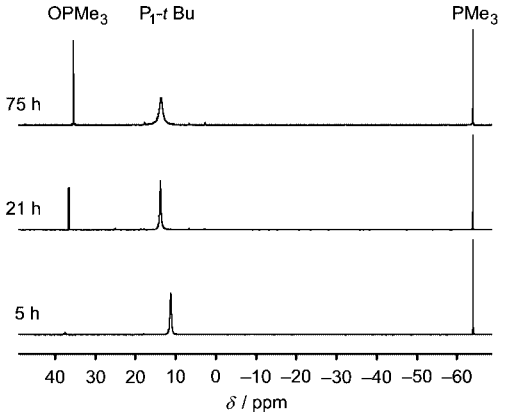

Figure 6. Selected $^{31}P\{^{1}H\}$ NMR spectra during catalysis.

diates of catalytic cycles will be further developed in our laboratories.

Experimental Section

Unless noted otherwise, all manipulations were carried out under anaerobic conditions by means of standard Schlenk techniques. For the solid-phase reactions a flask with a nitrogen inlet and a fritted glass filter with large pores that allows addition and removal of reagents and solvents without exposure of the resin to the atmosphere was used. All solvents were dried by standard methods and distilled under anaerobic conditions prior to use.

NMR: Bruker Avance DPX 200 at 200.15 MHz and Varian Unity Plus 400 at 399.89 MHz (^{1}H); chemical shifts (δ) in ppm with respect to residual solvent peaks as internal standard: $[D]_8THF$ (^{1}H: δ = 1.73, 3.58; ^{13}C: δ = 25.5, 67.7) or with respect to external 85% H_3PO_4 (^{31}P: δ = 0 ppm). CP MAS NMR: Bruker Avance 400 NMR with a 4 mm MAS probe head. IR: BioRad Excalibur FTS 3000 spectrometer using CsI disks. EI-MS, FAB-MS: Finnigan MAT 8400 spectrometer. – LIFDI-MS: JEOL JMS-700 double-focusing magnetic sector mass spectrometer.[37] UV/Vis: Perkin–Elmer Lambda 19, 0.2-cm cells (Hellma, suprasil). – Melting points: Gallenkamp capillary melting point apparatus MFB 595 010. – Elemental analyses: Microanalytical Laboratory of the Organic Chemistry Department, University of Heidelberg. – EPR: Bruker ELEXSYS E500 spectrometer (X-band). Xsophe, version 1.0.2β was used for simulation of the spectra using the following parameters: isotope ^{98}Mo (I = 0; 100%), ^{31}P, ^{1}H, $^{35,37}Cl$ natural isotope distribution; g- and A-strain Gaussian line shape model; matrix diagonalisation; 25 theta orientations; 5 field segments; orthorhombic symmetry. No attempts have been made for simulation of ^{95}Mo spectra or ^{95}Mo satellites.

Synthesis of 1a: The ligand (1.67 g, 6.5 mmol) dissolved in THF (10 mL) was added to a suspension of $MoCl_2O_2$(dme) (0.94 g, 3.24 mmol) in THF (40 mL) and triethylamine (0.9 mL, 6.5 mmol) was added. The red mixture was stirred at 25 °C for 1 h and heated under reflux for 2 h. After cooling to room temperature the mixture was filtered and the solvent was removed in vacuo. Toluene (40 mL) was added, covered with hexanes and the solution was cooled to 4 °C. The red precipitate was collected by filtration and dried. Yield 55% (2.31 g, 3.6 mmol); m.p. 168 °C; calcd. for $C_{28}H_{34}MoN_4O_4Si_2$ (642.7) C 52.33, H 5.33, N 8.72; found C 52.55, H 5.40, N 8.74. MS (EI): m/z (%) = 644 (98) $[M]^+$, 387 (11) $[M - C_{14}H_{17}N_2OSi]^+$, 257 (100) $[C_{14}H_{17}N_2OSi]$. HR-MS (EI): calcd. for ^{98}Mo 644.1177, found 644.1217; calcd. for ^{96}Mo 642.1176, found 642.1129; calcd. for ^{95}Mo 641.1181, found 641.1144. IR (CsI): $\tilde{\nu}$ = 2961 cm^{-1} (w), 1605 (m), 1585 (s), 1526 (m), 1499 (m), 1251 (s, C–O), 930 (m, Mo=O), 902 cm^{-1} (m, Mo=O). UV (THF): λ_{max} = 303 nm (43260 $M^{-1}cm^{-1}$), 440 nm (6130 $M^{-1}cm^{-1}$). ^{1}H NMR ($[D_8]$THF): δ = 7.94 (s, 1 H, H^7), 7.25 (s, 1 H, br. s, H^{11}), 6.97 (d, 2 H, ^{3}J = 8.5 Hz, $H^{2,6}$), 6.60 (d, 2 H, ^{3}J = 8.5 Hz, $H^{3,5}$), 6.39 (dvd, 1 H, ^{3}J = 3.4 Hz, 1.0 Hz, H^9), 6.11 (dvd, 1 H, ^{3}J = 3.4 Hz, 2.4 Hz, H^{10}), 0.23 (s, 9 H, CH_3); $^{13}C\{^{1}H\}$ NMR ($[D_8]$THF): δ = 158.1 (s, C^7), 153.8 (s, C^4), 148.6 (s, C^1), 142.9 (s, C^{11}), 139.4 (s, C^8), 123.1 (s, $C^{2,6}$), 120.3 (s, $C^{3,5}$), 119.6 (s, C^9), 114.8 (s, C^{10}), –0.35 (s, CH_3); assignments are based on 2D NMR spectra.

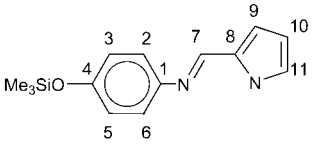

Synthesis of 2a: Complex **1a** (0.643 g, 1 mmol) was dissolved in THF (20 mL) and PMe_3 (1 M in THF, 0.6 mL, 0.6 mmol) was added. The reaction mixture was maintained at 50 °C for 12 h. The solvent was removed in vacuo and the residue was washed with diethyl ether giving a brown product. Yield 95% (0.60 g, 0.48 mmol). MS (FAB): m/z (%) = 1268 (3) $[M]^+$, 1011 (2) $[M - C_{14}H_{17}N_2OSi]^+$, 628 (72) $[M - C_{28}H_{34}MoN_4O_4Si_2]^+$. HR-MS (FAB): calcd. for $^{98}Mo/^{98}Mo$ 1272.2396, found 1272.2418; calcd. for $^{96}Mo/^{98}Mo$ 1270.2389, found 1270.2380; calcd. for $^{96}Mo/^{96}Mo$ 1268.2414, found 1268.2393. IR (CsI): $\tilde{\nu}$ = 2960 cm^{-1} (w), 1604 (s), 1581 (s), 1509 (s), 1493 (s), 1253 (s, C–O), 960 cm^{-1} (m, Mo=O). UV (THF): λ_{max} = 300 (81850 $M^{-1}cm^{-1}$), 468 (20990 $M^{-1}cm^{-1}$) 548 nm (11150 $M^{-1}cm^{-1}$). ^{1}H NMR ($[D_8]$THF): δ = 7.86 (s, 1 H, H^7), 7.73 (s, 1 H, $H^{7'}$), 7.63 (br. s, 1 H, $H^{11'}$), 7.12 (d, 2 H, ^{3}J = 8.5 Hz, $H^{2',6'}$), 6.98 (d, 2 H, ^{3}J = 8.5 Hz, $H^{2,6}$), 6.59 (d, 2 H, ^{3}J = 8.5 Hz, $H^{3,5}$), 6.54 (d, 2 H, ^{3}J = 8.5 Hz, $H^{3',5'}$), 6.43 (d, 1 H, ^{3}J = 3.1 Hz, $H^{9'}$), 6.37 (d, 1 H, ^{3}J = 3.1 Hz, H^9), 6.32 (dvd, 1 H, $H^{10'}$), 6.08 (br. s, 1 H, H^{11}), 5.80 (dvd, 1 H, H^{10}), 0.21 (s, 9 H, CH_3), 0.20 (s, 9 H, CH_3); assignments are based on 2D NMR spectra; low solubility prevented acquisition of ^{13}C NMR spectroscopic data.

Synthesis of 3a: Complex **1a** (0.643 g, 1 mmol) was dissolved in THF (20 mL) and PMe_3 (1 M in THF, 2 mL, 2 mmol) was added. The reaction mixture was maintained at 50 °C for 12 h. The solvent was removed in vacuo and the residue was washed with diethyl ether giving a green product. Yield 80% (0.562 g, 0.80 mmol); LIFDI-MS: m/z (%) = 704 (100) $[M]^+$, 627 (30) $[M - PMe_3]^+$. IR (CsI): $\tilde{\nu}$ = 2961 cm^{-1} (w), 2906 (w), 1604 (m), 1572 (s), 1506 (vs), 1266 (vs, C–O), 1253 (vs, C–O), 954 cm^{-1} (m, Mo=O). UV (THF): λ_{max} = 294 (26090 $M^{-1}cm^{-1}$), 345 (27970 $M^{-1}cm^{-1}$), 410 nm (sh, 9060 $M^{-1}cm^{-1}$), 478 (sh, 3170 $M^{-1}cm^{-1}$), 629 (1050 $M^{-1}cm^{-1}$). ^{1}H NMR ($[D_8]$THF): δ = 7.98 (d, 1 H, $^{4}J_{PH}$ = 2.8 Hz, H^7), 7.61 (br. s, 1 H, H^{11}), 7.50 (br. s, 1 H, $H^{7'}$), 7.22 (d, 2 H, ^{3}J = 8.8 Hz, $H^{3,5}$), 7.00 (d, 1 H, ^{3}J = 3.4 Hz, H^9), 6.73 (d, 2 H, ^{3}J = 8.8 Hz, $H^{2,6}$), 6.57 (s, 4 H, $H^{2',6',3',5'}$), 6.49 (dvd, 1 H, H^{10}), 6.30 (d, 1 H, ^{3}J = 3.4 Hz, $H^{9'}$), 5.80 (br. s, 1 H, $H^{11'}$), 5.78 (dvd, 1 H, $H^{10'}$), 1.29 (d, 9 H, $^{2}J_{PH}$ = 8.5 Hz, PMe_3), 0.29 (s, 9 H, CH_3), 0.24 (s, 9 H, CH_3); $^{13}C\{^{1}H\}$ NMR ($[D_8]$THF): δ = 158.0 (s, C^7), 150.6 (s, $C^{7'}$), 147.3 (s, C^{11}), 137.8 (s, $C^{11'}$), 158.0 (s, C^7), 125.0 (s, $C^{3,5}$), 124.1 (s, $C^{3',5'}$), 120.3 (s, $C^{2',6'}$), 119.9 (s, $C^{2,6}$), 118.9 (s, C^9), 115.2 (s, $C^{9'}$), 114.5 (s, C^{10}), 113.1 (s, $C^{10'}$), 16.2 (d, $^{1}J_{PC}$ = 23.3 Hz, PCH_3), 0.40 (s, CH_3), 0.39 (s, CH_3); assignments are based on 2D NMR spectra; low solubility prevented observation of C^1, C^4, C^8; $^{31}P\{^{1}H\}$ NMR ($[D_8]$THF): δ = 2.41 (s). ^{31}P NMR ($[D_8]$THF): δ = 2.41 (m, $^{2}J_{PH}$ = 8.5 Hz, $^{4}J_{PH}$ = 2.8 Hz).

Determination of Activation Parameters for OAT between 1a and PMe_3: In a typical experiment a UV cell containing a known amount of **1a** in THF was thermostatted at the desired temperature and 100 eq PMe_3 (1 M in THF) were added. The time dependence of the absorbance was measured at 548 nm.

Synthesis of 1b: The immobilised ligand (1.0 g, 0.8 mmol) was suspended in THF (30 mL) and $MoCl_2O_2$(dme) (116 mg, 0.4 mmol) was added as a solid. After 10 min triethylamine (0.28 mL, 2 mol) was added. The suspension was stirred at 25 °C for 1 h and heated under reflux for 2 h. After cooling to room temperature the mixture was filtered and washed successively with THF and diethyl ether giving a bright red resin. The isotopically enriched samples were prepared starting from $^{95}MoO_3$ (98% ^{95}Mo) via $Na_2{}^{95}MoO_4$ and $^{95}MoCl_2O_2$(dme).

Determination of Mo Uptake: 1.0 g (0.80 mmol) of immobilised ligand was treated as above with $MoCl_2O_2$(dme) (103.8 mg, 0.36 mmol). All washing solutions were collected, evaporated to dryness and dissolved in ethanol (50 mL). 4 mL of this solution were treated with a $3.3\cdot10^{-3}$ M solution of 5,7-dibromo-8-hydroxyquinoline (1 mL), 0.5 M H_2SO_4 (1 mL) and ethanol (4 mL). The solution was diluted with H_2O to 10 mL. Absorbance was measured at 400 nm and molybdenum content was determined using a calibration graph.[23] A(400 nm) = 1.432122 corresponds to 32.1 mg (0.11 mmol) $MoCl_2O_2$(dme), i.e. 0.25 mmol molybdenum was immobilised onto the polymer.[38]

Cleavage with [nBu$_4$N]F: To resin **1b** (500 mg, 0.13 mmol Mo) suspended in THF (10 mL) was added [nBu$_4$N]F·3H$_2$O (107 mg, 0.34 mol) dissolved in THF (10 mL). The solution immediately became coloured. The solution was collected by filtration and the solvents evaporated to dryness. The residue was washed with diethyl ether (to remove ammonium salts and free ligand) giving a red product. ^{1}H NMR ([D$_8$]THF): δ = 11.0 (br. s, 1 H, OH), 8.05 (s, 1 H, H^7), 7.13 (s, 1 H, br. s, H^{11}), 7.10 (d, 2 H, ^3J = 8.5 Hz, H^{2,6}), 6.66 (d, 2 H, ^3J = 8.5 Hz, H^{3,5}), 6.45 (d, 1 H, ^3J = 2.5 Hz, H^9), 6.15 (pt, 1 H, H^{10}).

Synthesis of 3b: To resin **1b** (300 mg, 0.08 mmol Mo) suspended in THF (10 mL) was added PMe_3 (1 M in THF, 0.2 mL, 0.2 mmol) and the mixture was held at 40 °C for 4 h. The $OPMe_3$ formed was detected by ^{31}P NMR spectroscopy. The resulting resin was washed with THF and diethyl ether giving a dark coloured resin. ^{31}P{^{1}H} CP-MAS NMR: δ = 2.4.

Reduction of 1b with Co(C_5H_5)$_2$: To resin **1b** (300 mg, 0.08 mmol Mo) suspended in THF (10 mL) was added Co(C_5H_5)$_2$ (19 mg, 0.1 mmol) and the mixture was held at 40 °C for 5 h. The resulting resin was washed with THF and diethyl ether giving a dark coloured resin **4b**. EPR (solid, 295 K): g_1 = 1.9544, g_2 = 1.9388, g_3 = 1.9111.

Oxidation of 3b with [Fe(C_5H_5)$_2$][BF_4]: To resin **3b** (300 mg, 0.08 mmol Mo) suspended in THF (10 mL) was added [Fe(C_5H_5)$_2$][PF_6] (33 mg, 0.1 mmol) and the mixture was held at 40 °C for 5 h. The resulting resin was washed with THF and diethyl ether giving a dark coloured resin **5b**. EPR (solid, 295 K): g_1 = 1.9812, g_2 = 1.9528, g_3 = 1.9415; A_1(^{31}P) = 23 G, A_2(^{31}P) = 27 G, A_3(^{31}P) = 23 G.

Reaction of 5b with H_2O: To resin **5b** (300 mg, 0.08 mmol Mo) suspended in THF (10 mL) was added H_2O (0.1 mL, 5.6 mmol) and the mixture was held at 25 °C for 18 h. The resulting resin was washed with THF and diethyl ether giving a dark coloured resin **6b**. EPR (solid, 295 K): g_1 = 1.9868, g_2 = 1.9624, g_3 = 1.9440; $A_1(2\times{}^1H)$ = 30 G, $A_2(2\times{}^1H)$ = 7 G, $A_3(2\times{}^1H)$ = 28 G.

Reaction of 5b with [nBu$_4$N]Cl: To resin **5b** (80 mg, 0.02 mmol Mo) suspended in THF (5 mL) was added [nBu$_4$N]Cl (28 mg, 0.1 mmol) and the mixture was held at 25 °C for 18 h. The resulting resin was washed with THF and diethyl ether giving a dark coloured resin **7b**. EPR (solid, 295 K): g_1 = 1.9680, g_2 = 1.9522, g_3 = 1.9362; A_1(^{35,37}Cl) = 7 G, A_2(^{35,37}Cl) = 10 G, A_3(^{35,37}Cl) = 8 G.[39]

Catalytic Experiments with 1b: To resin **1b** (50 mg, 0.013 mmol Mo) suspended in THF/CH_3CN (5 mL, 1 mL) was added PMe_3 (1 M in THF, 1 mL, 1 mmol), P_1-tBu (0.5 mL, 2 mmol), H_2O (0.030 mL, 1.6 mmol) and [Fe(AcC_5H_4)$_2$][BF_4] (714 mg, 2 mmol) and the mixture was held at 35 °C. ^{31}P{^{1}H} NMR spectra of the solution indicated selective formation of $OPMe_3$. The ^{1}H NMR spectrum of the solution after 126 h displays signals for $OPMe_3$ (δ = 1.35 ppm, d, $^2J_{PH}$ = 13.1 Hz), residual PMe_3 (δ = 0.90 ppm, d, $^2J_{PH}$ = 2.2 Hz), P_1-tBu (δ = 2.63, 2.59, 1.17 ppm), H_2O (δ = 2.80 ppm) and Fe(AcC_5H_4)$_2$ (δ = 4.71, 4.46, 2.22 ppm).

The EI mass spectra of the dried residue show signals for Fe(AcC_5H_4)$_2$ (m/z = 270, 255, 227, 199, 163), P_1-tBu (m/z = 234, 219) and $OPMe_3$ (m/z = 92, 77). Using ^{18}O-labeled water (95% ^{18}O) the EI mass spectra display peaks for $^{18}OPMe_3$ (m/z = 94, 79). Additionally the mass spectra indicate incorporation of the ^{18}O label into Fe(AcC_5H_4)$_2$ (m/z = 272 [single ^{18}O; 36.10%], 274 [double ^{18}O, 6.1%]), probably by hydrating the ketone groups and dehydrating the geminal diol. This reduces the fraction of $H_2{}^{18}O$ present during catalysis from 95% to 40 ± 12% as calculated from the amount of ^{16}O released from Fe(AcC_5H_4)$_2$, the amount of ^{16}O present in the catalyst and in the water employed. The fraction of $^{18}OPMe_3$ was calculated as 33.1% from the mass spectroscopic analysis agreeing within error with the expected value.

Supporting Information (see also the footnote on the first page of this article): The Supporting Information contains the LIFDI-MS spectrum of **3a** and molecular ion peak, the UV/Vis absorption spectra of **1a** and 100 eq PMe_3 at 60 °C, the calibration graph for Mo uptake, the EPR spectrum of **5b** at 295 K and simulation, the EPR spectrum of **6b** at 295 K and simulation, the EPR spectrum of **7b** at 295 K and simulation, the conversion vs. time plot, the ^{1}H NMR spectrum after 126 h and the partial EI mass spectra of the reaction products.

Acknowledgments

This work was supported by the Deutsche Forschungsgemeinschaft (DFG, German Research Foundation) (Collaborative Research Center 623). K. H. gratefully acknowledges a Heisenberg fellowship from the German Science Foundation. We thank Prof. J. Blümel (Heidelberg) for measuring the CP MAS ^{31}P{^{1}H} NMR spectrum and Dr. J. Gross (Heidelberg) for the LIFDI mass spectra.

[1] A complete issue of *Chemical Reviews* is devoted to the subject "*Biomimetic Inorganic Chemistry*": *Chem. Rev.* **2004**, *104*, 347–1200.
[2] R. Hille, *Chem. Rev.* **1996**, *96*, 2757–2816.
[3] J. H. Enemark, C. G. Young, *Adv. Inorg. Chem.* **1993**, *40*, 1–88.
[4] C. G. Young, in: *Biomimetic Oxidations Catalyzed by Transition Metals* (Ed.: B. Meunier), Imperial College Press, London, **2004**, pp. 415–459.
[5] J. H. Enemark, J. J. A. Cooney, J. J. Wang, R. H. Holm, *Chem. Rev.* **2004**, *104*, 1175–1200.
[6] J. M. Tunney, J. McMaster, D. C. Garner, in: *Comprehensive Coordination Chemistry II*, vol. 8 (Eds.: J. A. McCleverty, T. J. Meyer), Elsevier Pergamon, Amsterdam, **2004**, pp. 459–477.
[7] R. H. Holm, *Coord. Chem. Rev.* **1990**, *100*, 183–221.

[8] J. Jiang, R. H. Holm, *Inorg. Chem.* **2005**, *44*, 1068–1072.
[9] F. Jalilehvand, B. S. Lim, R. H. Holm, B. Hedman, K. O. Hodgson, *Inorg. Chem.* **2003**, *42*, 5531–5536.
[10] K.-M. Sung, R. H. Holm, *J. Am. Chem. Soc.* **2002**, *124*, 4312–4320.
[11] K.-M. Sung, R. H. Holm, *J. Am. Chem. Soc.* **2001**, *123*, 1931–1943.
[12] B. S. Lim, R. H. Holm, *J. Am. Chem. Soc.* **2001**, *123*, 1920–1930.
[13] C. J. Doonan, D. A. Slizys, C. G. Young, *J. Am. Chem. Soc.* **1999**, *121*, 6430–6436.
[14] J. A. Craig, R. H. Holm, *J. Am. Chem. Soc.* **1989**, *111*, 2111–2115.
[15] J. M. Berg, R. H. Holm, *J. Am. Chem. Soc.* **1985**, *107*, 925–932.
[16] S. F. Gheller, B. E. Schultz, M. J. Scott, R. H. Holm, *J. Am. Chem. Soc.* **1992**, *114*, 6934–6935.
[17] R. H. Holm, J. M. Berg, *Acc. Chem. Res.* **1986**, *19*, 363–370.
[18] V. N. Nemykin, P. Basu, *Inorg. Chem.* **2005**, *44*, 7494–7502.
[19] A. J. Millar, C. J. Doonan, P. D. Smith, V. N. Nemykin, P. Basu, C. G. Young, *Chem. Eur. J.* **2005**, *11*, 3255–3267.
[20] Z. Xiao, M. A. Bruck, J. H. Enemark, C. G. Young, A. G. Wedd, *Inorg. Chem.* **1996**, *35*, 7508–7515.
[21] Z. Xiao, M. A. Bruck, C. Doyle, J. H. Enemark, C. Grittini, R. W. Gable, A. G. Wedd, C. G. Young, *Inorg. Chem.* **1995**, *34*, 5950–5962.
[22] Probably due to the smaller cone angle of PMe_3 (118°) as compared to that of PPh_3 (145°): C. A. Tolman, *Chem. Rev.* **1977**, *77*, 313–348.
[23] See supporting information for details.
[24] K. Most, J. Hoßbach, D. Vidović, J. Magull, N. C. Mösch-Zanetti, *Adv. Synth. Catal.* **2005**, *347*, 463–472.
[25] M. S. Reynolds, J. M. Berg, R. H. Holm, *Inorg. Chem.* **1984**, *23*, 3057–3062.
[26] K is strongly correlated to ε_{548} of **2a** thus fits of similar quality are possible for different combinations of ε_{548} and K[25] but reasonable combinations are $\varepsilon_{548} = 9000 \pm 3000$ $M^{-1}cm^{-1}$ and $K = 2 \pm 1\ 10^5$ M^{-1}. The rate constant k is well defined by the time of maximum absorbance.
[27] S. Reinhardt, K. Heinze, *Z. Anorg. Allg. Chem.* **2006**, 1465–1470.
[28] K. Heinze, V. Jacob, C. Feige, *Eur. J. Inorg. Chem.* **2004**, 2053–2061.
[29] K. Heinze, J. B. Toro, *Eur. J. Inorg. Chem.* **2004**, 3498–3507.
[30] K. Heinze, J. B. Toro, *Angew. Chem.* **2003**, *115*, 4671–4674; *Angew. Chem. Int. Ed.* **2003**, *42*, 4533–4536.
[31] K. Heinze, *Chem. Eur. J.* **2001**, *7*, 2922–2932.
[32] K. Heinze, U. Winterhalter, T. Jannack, *Chem. Eur. J.* **2000**, *6*, 4203–4210.
[33] For redox potentials see: N. G. Connelly, W. E. Geiger, *Chem. Rev.* **1996**, *96*, 877–910.
[34] K. Heinze, A. Reinhardt, *Inorg. Chem.* **2006**, *45*, 2695–2703.
[35] Singly polymer attached Mo^V complexes have been prepared directly from Mo^V salts. As expected, anisotropic EPR spectra are obtained in the dry state: J. Topich, *Inorg. Chem.* **1982**, *21*, 2079–2082.
[36] R. Schwesinger, *Nachr. Chem. Tech. Lab.* **1990**, *38*, 1214–1226.
[37] J. H. Gross, N. Nieth, H. B. Linden, U. Blumbach, F. J. Richter, M. E. Tauchert, R. Tompers, P. Hofmann, *Anal. Bioanal. Chem.* **2006**, *386*, 52–58.
[38] M. J. Ahmed, M. E. Haque, *Anal. Sci.* **2002**, *18*, 433–439.
[39] We are aware that extraction of six parameters from a broad EPR signal is rather difficult and the values given should be taken with care. However, it was not possible to simulate the EPR signal without assumption of coupling to an $I = {}^3/_2$ nucleus ($^{35,37}Cl$).

Received: November 27, 2006
Published Online: January 15, 2007

